J|A|C|S
ARTICLES

Published on Web 04/26/2008

Crystallographic Characterization of Helical Secondary Structures in α/β-Peptides with 1:1 Residue Alternation

Soo Hyuk Choi, Ilia A. Guzei, Lara C. Spencer, and Samuel H. Gellman*

Department of Chemistry, University of Wisconsin, Madison, Wisconsin 53706

Received January 17, 2008; E-mail: gellman@chem.wisc.edu

Abstract: Oligomers that contain both α- and β-amino acid residues in a 1:1 alternating pattern have recently been shown by several groups to adopt helical secondary structures in solution. The β-residue substitution pattern has a profound effect on the type of helix formed and the stability of the helical conformation. On the basis of two-dimensional NMR data, we have previously proposed that β-residues with a five-membered ring constraint promote two different types of α/β-peptide helix. The "11-helix" contains *i*,*i*+3 C=O···H−N hydrogen bonds between backbone amide groups; these hydrogen bonds occur in 11-atom rings. The α/β-peptide "14/15-helix" contains *i*,*i*+4 C=O···H−N hydrogen bonds, which occur in alternating 14- and 15-atom rings. Here we provide crystallographic data for 14 α/β-peptides that form the 11-helix and/or the 14/15-helix. These results were obtained for a series of oligomers containing β-residues derived from (*S*,*S*)-*trans*-2-aminocyclopentanecarboxylic acid (ACPC) and α-residues derived from α-aminoisobutyric acid (Aib) or L-alanine (Ala). The crystallized α/β-peptides range in length from 4 to 10 residues. Nine of the α/β-peptides display the 11-helix in the solid state, three display the 14/15-helix, and two display conformations that contain both *i*,*i*+3 and *i*,*i*+4 C=O···H−N hydrogen bonds, but not bifurcated hydrogen bonds. Only 3 of the 14 crystal structures presented here have been previously described. These results suggest that longer α/β-peptides prefer the 14/15-helix over the 11-helix, a conclusion that is consistent with previously reported NMR data obtained in solution.

Introduction

The broad array of activities manifested among folded biopolymers (proteins and RNA) has inspired widespread interest in unnatural oligomers that display comparable folding behavior, which are collectively designated "foldamers".[1] A long-range goal of foldamer research is to endow synthetic oligomers with sophisticated functions of the types found among biopolymers or comparably sophisticated functions that are not part of the biopolymer repertoire. Efficient catalysis, selective recognition, programmed self-assembly, and other natural protein activities often require adoption of a specific conformation by the polypeptide backbone, and it seems likely that function-based engineering of foldamers will depend upon a thorough understanding of the conformational propensities of unnatural backbones. β-Peptides (oligomers of β-amino acids) are among the most widely studied foldamers at present, and there are now many examples in which β-peptide function requires the adoption of a discrete and predictable secondary structure.[2]

Our ability to achieve specific functional goals with foldamers should be enhanced by enlarging the set of backbones for which folding rules are known, because each new scaffold offers new ways to orient sets of side chains in space. Proteins have homogeneous backbones, since all building blocks come from a single class (α-amino acids). A desire to move beyond the biopolymer prototypes has recently motivated many researchers to explore oligomers with heterogeneous backbones, that is, backbones containing more than one type of building block.[3–9] Several groups have characterized the folding of oligomers containing both α- and β-amino acid residues ("α/β-peptides").[3–6] A number of helical secondary structures have been computationally predicted[5] and/or empirically deduced based on NMR

(1) (a) Gellman, S. H. *Acc. Chem. Res.* **1998**, *31*, 173. (b) Hill, D. J.; Mio, M. J.; Prince, R. B.; Hughes, T. S.; Moore, J. S. *Chem. Rev.* **2001**, *101*, 3893–4011. (c) Hecht, S., Huc, I., Eds. *Foldamers: Structure, Properties and Applications*; Wiley-VCH: Weinheim, Germany, 2007. (d) Goodman, C. M.; Choi, S.; Shandler, S.; DeGrado, W. F. *Nat. Chem. Biol.* **2007**, *3*, 252.

(2) (a) Cheng, R. P.; Gellman, S. H.; DeGrado, W. F. *Chem. Rev.* **2001**, *101*, 3219. (b) Stephens, O. M.; Kim, S.; Welch, B. D.; Hodsdon, M. E.; Kay, M. S.; Schepartz, A. *J. Am. Chem. Soc.* **2005**, *127*, 13126. (c) Potocky, T. B.; Menon, A. K.; Gellman, S. H. *J. Am. Chem. Soc.* **2005**, *127*, 3686. (d) English, E. P.; Chumanov, R. S.; Gellman, S. H.; Compton, T. *J. Biol. Chem.* **2006**, *281*, 2661. (e) Pomerantz, W. C.; Abbott, N. L.; Gellman, S. H. *J. Am. Chem. Soc.* **2006**, *128*, 8730. (f) Karlsson, A. J.; Pomerantz, W. C.; Weisblum, B.; Gellman, S. H.; Palecek, S. P. *J. Am. Chem. Soc.* **2006**, *128*, 12630.

(3) (a) Hayen, A.; Schmitt, M. A.; Ngassa, F. N.; Thomasson, K. A.; Gellman, S. H. *Angew. Chem., Int. Ed.* **2004**, *43*, 505. (b) Schmitt, M. A.; Weisblum, B.; Gellman, S. H. *J. Am. Chem. Soc.* **2004**, *126*, 6848. (c) Schmitt, M. A.; Choi, S. H.; Guzei, I. A.; Gellman, S. H. *J. Am. Chem. Soc.* **2005**, *127*, 13130. (d) Sadowsky, J. D.; Schmitt, M. A.; Lee, H.-S.; Umezawa, N.; Wang, S.; Tomita, Y.; Gellman, S. H. *J. Am. Chem. Soc.* **2005**, *127*, 11966. (e) Schmitt, M. A.; Choi, S. H.; Guzei, I. A.; Gellman, S. H. *J. Am. Chem. Soc.* **2006**, *128*, 4538. (f) Sadowsky, J. D.; Fairlie, W. D.; Hadley, E. B.; Lee, H. S.; Umezawa, N.; Nikolovska-Coleska, Z.; Wang, S. M.; Huang, D. C. S.; Tomita, Y.; Gellman, S. H. *J. Am. Chem. Soc.* **2007**, *129*, 139. (g) Schmitt, M. A.; Weisblum, B.; Gellman, S. H. *J. Am. Chem. Soc.* **2007**, *129*, 417. (h) Horne, W. S.; Price, J. L.; Keck, J. L.; Gellman, S. H. *J. Am. Chem. Soc.* **2007**, *129*, 4178. (i) Price, J. L.; Horne, W. S.; Gellman, S. H. *J. Am. Chem. Soc.* **2007**, *129*, 6376. (j) Choi, S. H.; Guzei, I. A.; Gellman, S. H. *J. Am. Chem. Soc.* **2007**, *129*, 13780. (k) Horne, W. S.; Boersma, M. D.; Windsor, M. A.; Gellman, S. H. Angew. Chem. Int. Ed., Early View (DOI: 10.1002/anie.200705315).

10.1021/ja800355p CCC: $40.75

analysis.[3a,b,4] Our own efforts in this area have focused on conformationally restricted β-residues, such as those derived from *trans*-2-aminocyclopentanecarboxylic acid (ACPC).[10] For α/β-peptides with 1:1 residue alternation, we have found that the five-membered ring constraint favors two different helical conformations that are named on the basis of the characteristic hydrogen bonds formed between backbone amide groups.[3a] The 11-helix contains *i*,*i*+3 C=O···H−N hydrogen bonds, and the 14/15-helix contains *i*,*i*+4 C=O···H−N hydrogen bonds. These two α/β-peptide helices can be regarded as analogues of the two most common helical secondary structures among proteins, the 3_{10}-helix (*i*,*i*+3 C=O···H−N hydrogen bonds) and the α-helix (*i*,*i*+4 C=O···H−N hydrogen bonds). Relatively short α/β-peptides containing constrained β-residues (6−8 residues total) appear to form both helices in solution, with interconversion rapid on the NMR time scale. Longer α/β-peptides in this family (15 residues) seem to favor the 14/15-helix in solution.[3b] However, these NMR-based conclusions must be regarded as tentative because all α/β-peptides examined to date experience rapid equilibration between folded and unfolded states on the NMR time scale.

Chart 1. Crystallized α/β-Peptides

4 Boc-Aib-ACPC-Aib-ACPC-OBn

5 Boc-Aib-ACPC-Aib-ACPC-Aib-OBn

6 Boc-Aib-ACPC-Aib-ACPC-Aib-ACPC-OBn
6a Boc-Ala-ACPC-Aib-ACPC-Aib-ACPC-OBn
6b Boc-Aib-ACPC-Ala-ACPC-Aib-ACPC-OBn

7 Boc-Aib-ACPC-Aib-ACPC-Aib-ACPC-Aib-OBn
7a Boc-Ala-ACPC-Aib-ACPC-Aib-ACPC-Aib-OBn

8 Boc-Aib-ACPC-Aib-ACPC-Aib-ACPC-Aib-ACPC-OBn
8a Boc-Ala-ACPC-Ala-ACPC-Aib-ACPC-Aib-ACPC-OBn
8b Boc-Ala-ACPC-Aib-ACPC-Aib-ACPC-Aib-ACPC-OBn
8c Boc-Ala-ACPC-Aib-ACPC-Ala-ACPC-Aib-ACPC-OBn

9 Boc-Ala-ACPC-Aib-ACPC-Aib-ACPC-Aib-ACPC-Aib-OBn
9a Boc-Ala-ACPC-Aib-ACPC-Ala-ACPC-Aib-ACPC-Aib-OBn

10 Boc-Ala-ACPC-Ala-ACPC-Aib-ACPC-Aib-ACPC-Aib-ACPC-OBn

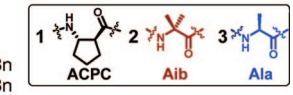

Crystallographic data for new foldamers provide high-resolution structural information that serves as a basis for subsequent function-based design efforts. To date, only three crystal structures have been reported for α/β-peptides with 1:1 residue alternation.[3c,j] Here we report an additional 11 α/β-peptide crystal structures, in which all β-residues are (*S,S*)-ACPC (**1**) and the α-residues are α-aminoisobutyric acid (Aib; **2**) or L-alanine (Ala; **3**). Chart 1 shows all 14 α/β-peptides for which crystal structures have been obtained (the structures of **8**, **8b**, and **9** have been previously described).[3c,e] The α/β-peptides range in length from 4 to 10 residues, and length seems to influence the type of helix formed in the solid state. Up to the heptamer length, the α/β-peptides crystallize in the 11-helical conformation. Among the four octamers we crystallized, two are entirely 11-helical; that is, they contain exclusively *i*,*i*+3 C=O···H−N hydrogen bonds. The other two display helical conformations that contain both *i*,*i*+3 and *i*,*i*+4 C=O···H−N hydrogen bonds. The two nonamers and the decamer crystallize in the 14/15-helical conformation; that is, they display only *i*,*i*+4 C=O···H−N hydrogen bonds. The resulting set of structures is large enough to allow a meaningful analysis of the α-residue and β-residue torsion angles associated with each type of helix.

Results and Discussion

Synthesis. A previously reported procedure[10b,c] was used to prepare the ACPC derivative 2-(1-phenylethylamino)cyclopentanecarboxylic acid ethyl ester. The phenylethyl group was removed via catalytic hydrogenolysis, and the resulting amino group was acylated with Boc-Ala-OH or Boc-Aib-OH using a carbodiimide activating agent. The resulting dipeptide ethyl esters, Boc-Ala-ACPC-OEt and Boc-Aib-ACPC-OEt, were either saponified or converted directly to the benzyl ester. All α/β-peptides in Chart 1 were prepared by carbodiimide-mediated coupling of dipeptide segments.

α/β-Peptide Crystal Structures. 11-Helical conformations are adopted in the solid state by the α/β-peptides among our set that contain from four to seven residues (Figure 1). Tetramer **4** and pentamer **5**, with alternating Aib and ACPC residues, display the maximum number of 11-membered H-bonded rings. For each of the three hexamers (**6**, **6a**, and **6b**) the N-terminal α-residue does not participate in the helical hydrogen bonding pattern, although the rest of each hexamer is 11-helical. Heptamer **7**, which contains only Aib α-residues, adopts a fully

(4) (a) De Pol, S.; Zorn, C.; Klein, C. D.; Zerbe, O.; Reiser, O. *Angew. Chem., Int. Ed.* **2004**, *43*, 511. (b) Sharma, G. V. M.; Nagendar, P.; Jayaprakash, P.; Krishna, P. R.; Ramakrishna, K. V. S.; Kunwar, A. C. *Angew. Chem., Int. Ed.* **2005**, *44*, 5878. (c) Srinivasulu, G.; Kumar, S. K.; Sharma, G. V. M.; Kunwar, A. C. *J. Org. Chem.* **2006**, *71*, 8395. (d) Seebach, D.; Jaun, B.; Sebesta, R.; Mathad, R. I.; Flogel, O.; Limbach, M.; Sellner, H.; Cottens, S. *Helv. Chim. Acta* **2006**, *89*, 1801. (e) Vilaivan, T.; Srisuwannaket, C. *Org. Lett.* **2006**, *8*, 1897. (f) Jagadeesh, B.; Prabhakar, A.; Sarma, G. D.; Chandrasekhar, S.; Chandrashekar, G.; Reddy, M. S.; Jagannadh, B. *Chem. Commun.* **2007**, 371.

(5) (a) Baldauf, C.; Gunther, R.; Hofmann, H. J. *Biopolymers* **2006**, *84*, 408. (b) Zhu, X.; Yethiraj, A.; Cui, Q. *J. Chem. Theory Comput.* **2007**, *3*, 1538.

(6) For crystal structures of short α/β-peptides: (a) Karle, I. L.; Handa, B. K.; Hassall, C. H. *Acta Crystallogr., Sect. B: Struct. Sci.* **1975**, *B31*, 555. (b) Pavone, V.; Diblasio, B.; Lombardi, A.; Isernia, C.; Pedone, C.; Benedetti, E.; Valle, G.; Crisma, M.; Toniolo, C.; Kishore, R. *J. Chem. Soc., Perkin Trans. 2* **1992**, 1233. (c) Hanessian, S.; Yang, H. *Tetrahedron Lett.* **1997**, *38*, 3155. (d) Rossi, F.; Bucci, E.; Isernia, C.; Saviano, M.; Iacovino, R.; Romanelli, A.; Di Lello, P.; Grimaldi, M.; Montesarchio, D.; De Napoli, L.; Piccialli, G.; Benedetti, E. *Biopolymers* **2000**, *53*, 140. (e) Tanaka, M.; Oba, M.; Ichiki, T.; Suemune, H. *Chem. Pharm. Bul.* **2001**, *49*, 1178.

(7) (a) Hagihara, M.; Anthony, N. J.; Stout, T. J.; Clardy, J.; Schreiber, S. L. *J. Am. Chem. Soc.* **1992**, *114*, 6568. (b) Baldauf, C.; Gunther, R.; Hofmann, H. J. *J. Org. Chem.* **2006**, *71*, 1200. (c) Sharma, G. V. M.; Jadhav, V. B.; Ramakrishna, K. V. S.; Narsimulu, K.; Subash, V.; Kunwar, A. C. *J. Am. Chem. Soc.* **2006**, *128*, 14657. (d) Baruah, P. K.; Sreedevi, N. K.; Gonnade, R.; Ravindranathan, S.; Damodaran, K.; Hofmann, H. J.; Sanjayan, G. J. *J. Org. Chem.* **2007**, *72*, 636. (e) Vasudev, P. G.; Ananda, K.; Chatterjee, S.; Aravinda, S.; Shamala, N.; Balaram, P. *J. Am. Chem. Soc.* **2007**, *129*, 4039. (f) Chatterjee, S.; Roy, R. S.; Balaram, P. *J. R. Soc. Interface* **2007**, *4*, 587.

(8) (a) Gong, B. *Proc. Natl. Acad. Sci. U.S.A.* **2002**, *99*, 11583. (b) Yang, D.; Li, W.; Qu, J.; Luo, S. W.; Wu, Y. D. *J. Am. Chem. Soc.* **2003**, *125*, 13018. (c) Chowdhury, S.; Schatte, G.; Kraatz, H. B. *Angew. Chem., Int. Ed.* **2006**, *45*, 6882. (d) Zhao, Y.; Zhong, Z. Q.; Ryu, E. H. *J. Am. Chem. Soc.* **2007**, *129*, 218. (e) Olsen, C. A.; Bonke, G.; Vedel, L.; Adsersen, A.; Witt, M.; Franzhk, H.; Jaroszewski, J. W. *Org. Lett.* **2007**, *9*, 1549. (f) Angelici, G.; Luppi, G.; Kaptein, B.; Broxterman, Q. B.; Hofmann, H. J.; Tomasini, C. *Eur. J. Org. Chem.* **2007**, 2713. (g) Zhong, Z.; Zhao, Y. *Org. Lett.* **2007**, *9*, 2891. (h) Delsuc, N.; Godde, F.; Kauffmann, B.; Leger, J. M.; Huc, I. *J. Am. Chem. Soc.* **2007**, *129*, 11348.

(9) For α/β-peptides with sheet or turn structures, see:(a) Krauthauser, S.; Christianson, L. A.; Powell, D. R.; Gellman, S. H. *J. Am. Chem. Soc.* **1997**, *119*, 11719. (b) Huck, B. R.; Fisk, J. D.; Gellman, S. H. *Org. Lett.* **2000**, *2*, 2607. (c) Gopi, H. N.; Roy, R. S.; Raghothama, S. R.; Karle, I. L.; Balaram, P. *Helv. Chim. Acta* **2002**, *85*, 3313. (d) Arnold, U.; Hinderaker, M. P.; Nilsson, B. L.; Huck, B. R.; Gellman, S. H.; Raines, R. T. *J. Am. Chem. Soc.* **2002**, *124*, 8522. (e) Roy, R. S.; Karle, I. L.; Ragothama, S.; Balaram, P. *Proc. Natl. Acad. Sci U.S.A.* **2004**, *101*, 16478. (f) Roy, R. S.; Gopi, H. N.; Ragothama, S.; Karle, I. L.; Balaram, P. *Chem.−Eur. J.* **2006**, *12*, 3295.

(10) (a) Appella, D. H.; Christianson, L. A.; Klein, D. A.; Richards, M. R.; Powell, D. R.; Gellman, S. H. *J. Am. Chem. Soc.* **1999**, *121*, 7574. (b) Lee, H.-S.; LePlae, P. L.; Porter, E. A.; Gellman, S. H. *J. Org. Chem.* **2001**, *66*, 3597. (c) LePlae, P. R.; Umezawa, N.; Lee, H.-S.; Gellman, S. H. *J. Org. Chem.* **2001**, *66*, 5629.

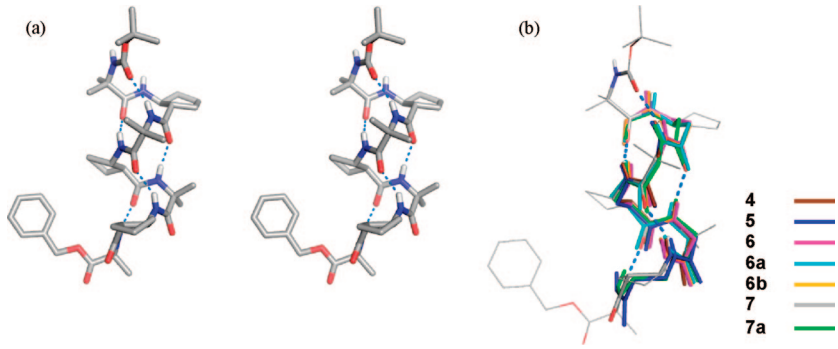

Figure 1. Crystal structures of 11-helical α/β-peptides: (a) stereoview of heptamer **7**. Hydrogen atoms other than amide protons are omitted. Dotted line indicates intramolecular H-bonds. (b) Overlay of seven structures. The structure of heptamer **7** is drawn in gray. For the other six structures, only backbone atoms (C_α, C_β, C═O, N−H) are shown. C-Terminal ACPCs and nonhelical N-terminal residues (in **6**, **6a**, **6b**) are omitted.

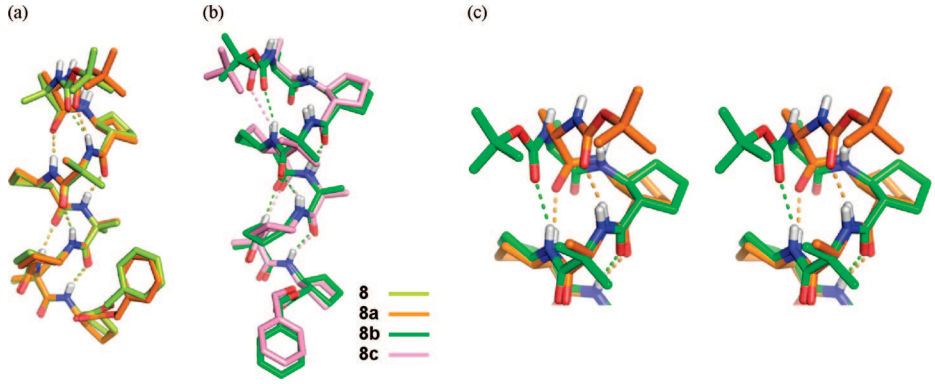

Figure 2. Crystal structures of octamers: (a) fully 11-helical conformation; (b) chimeric conformation (four 11-helical H-bonds and one 14-atom H-bonded ring). (c) Comparison of 11-atom and 14-atom H-bonded rings in **8a** and **8b**, respectively (stereoview). Only the first four residues from the N-terminus are shown.

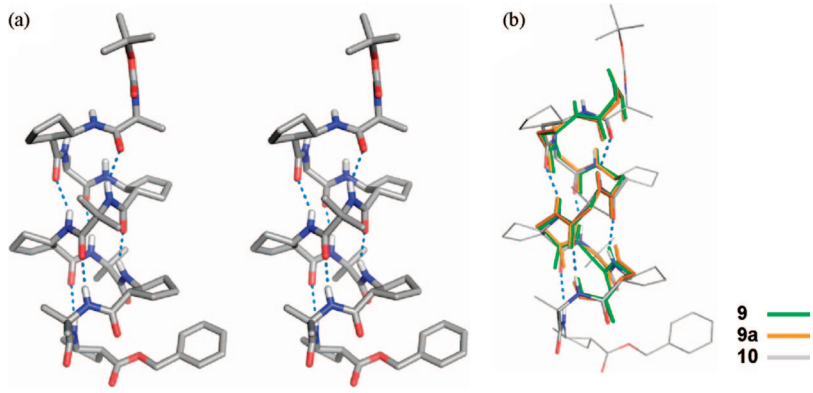

Figure 3. Crystal structures of 14/15-helical α/β-peptides: (a) stereoview of decamer **10**; (b) overlay of three structures. The structure of decamer **10** is drawn in gray. For the two nonamers, only backbone atoms (C_α, C_β, C═O, N−H) are shown.

11-helical conformation (five intramolecular hydrogen bonds). Heptamer **7a**, on the other hand, forms only four 11-helical hydrogen bonds in the solid state because the N-terminal Ala residue is not part of the helix, which parallels the behavior of the N-terminal α-residues in the three hexamers.

Among the four octamers, **8** and **8a** are fully 11-helical in the solid state (all six of the possible *i*,*i*+3 C═O···H−N hydrogen bonds are formed), while **8b** and **8c** display conformations that contain both 11-helical and 14/15-helical hydrogen bonds (Figure 2). Octamers **8b** and **8c** contain only four 11-helical hydrogen bonds in the solid state. For **8b**, the carbonyl of the N-terminal Boc group is engaged in a 14-membered ring hydrogen bond with the amide proton of ACPC-4 (*i*,*i*+4 C═O···H−N), which represents the beginning of a 14/15-helix. A similar interaction seems to occur in **8c**, but in this case the O···H distance, 2.7 Å, is a little longer than expected for a hydrogen bond. The N−H···O angle for this interaction is favorable (147°).

The three longest among our α/β-peptides, which contain 9 or 10 residues (**9**, **9a**, and **10**), display 14/15-helical conformations in the solid state (Figure 3). Nonamers **9** and **9a** are 14/15-helical: five and six *i*,*i*+4 C═O···H−N hydrogen bonds are evident, respectively. Decamer **10**, too, contains six *i*,*i*+4 C═O···H−N hydrogen bonds; formation of the seventh is precluded because the N-terminal Ala residue curls away from the helix in the solid state. This N-terminal α-residue distortion is similar to those observed for hexamers **6**, **6a**, and **6b** and heptamer **7**.

Implications from the Crystallographic Data Regarding Helical Folding in Solution. Our initial studies of α/β-peptides containing ACPC and similarly constrained β-residues focused on hexamers and octamers.[3a] These molecules were studied in solution, and two-dimensional NMR data were used to elucidate conformational behavior. Numerous medium-range NOEs were observed for pairs of protons from residues not adjacent in sequence, which provided strong evidence for helix formation in methanol solution. However, accommodating all of the *i*,*i*+2, *i*,*i*+3, and *i*,*i*+4 NOE patterns within a single helix was possible only by proposing a network of three-center or "bifurcated" hydrogen bonds, involving simultaneous *i*,*i*+3 and *i*,*i*+4 C═O···H−N interactions. Alternatively, we could account for the observed NOEs by proposing that two distinct helical conformations were populated, one containing only *i*,*i*+3 C═O···H−N hydrogen bonds (the 11-helix) and the other containing only *i*,*i*+4 C═O···H−N hydrogen bonds (the 14/15-helix), with rapid interconversion between these two helical conformations on the NMR time scale. We favored the latter hypothesis based on two considerations. First, bifurcated hydrogen bonds are rare in α-peptide and protein helices.[11] Second, interconversion between *i*,*i*+3 and *i*,*i*+4 C═O···H−N hydrogen bonding patterns, i.e., between the 3_{10}- and α-helices, has been reported for α-peptides.[12] However, the NMR data did not allow us to disprove either of these competing hypotheses.

The 14 α/β-peptide crystal structures reported here provide strong albeit indirect support for the hypothesis that α/β-peptides in solution can interconvert between 11- and 14/15-helical conformations rather than adopting a hybrid helical conformation that contains bifurcated hydrogen bonds. If one uses a standard structural criterion for identifying hydrogen bonds in the solid state, O···H 2.5 Å,[13] then there is not a single intramolecular bifurcated interaction among the 14 structures. If one relaxes this constraint slightly, to include O···H distances up to 2.8Å, then there is one possible bifurcated interaction at the C-terminus of nonamer **9** and another at the C-terminus of **9a**. Overall, the set of crystal structures suggests that forming two-center O···H interactions is strongly preferable to forming three-center interactions, even when the backbone seems to have trouble deciding between the *i*,*i*+3 and *i*,*i*+4 C═O···H−N hydrogen-bonding patterns (cf. structures of **8b** and **8c**).

Relationship between α/β-Peptide Length and Helix Preference. We have previously examined two 15-mer α/β-peptides by two-dimensional NMR, and in both cases the set of medium-range NOEs observed suggested that only the 14/15-helical conformation was populated to a significant extent.[3b,g] These results contrasted with previous conclusions based on the NOEs displayed by shorter α/β-peptides, which implied that both the 11- and 14/15-helical conformations are significantly populated. This contrast led us to propose that the 14/15-helix is increasingly favored relative to the 11-helix as the α/β-peptide backbone grows longer. A comparable helix preference trend is known among α-peptides: the α-helix (*i*,*i*+4 hydrogen bonds) is favored over the 3_{10}-helix (*i*,*i*+3 hydrogen bonds) by increasing the number of residues.[12a] This α-peptide preference has been suggested to arise from a competition between a drive to form the maximum number of intramolecular hydrogen bonds (favored by the smaller hydrogen-bonded ring) and a drive to minimize backbone conformational energy (apparently favored by the larger hydrogen-bonded ring).

Table 1. Average Interproton Distances (Å) Corresponding to Medium-Range NOE Patterns

	11-helix		14/15-helix	
NOE type	NOE[a]	crystal[b]	NOE[a]	crystal[b]
β-residue $C_\beta H(i)$−β-residue NH(i+2)	yes	3.2(22)	yes	4.2(12)
β-residue $C_\beta H(i)$−β-residue $C_\alpha H$ (i+2)	yes	2.9(22)	yes	3.9(11)
β-residue $C_\alpha H(i)$−β-residue NH(i+2)	yes	4.2(22)	yes	4.2(11)
α-residue $C_\alpha H(i)$−α-residue NH(i+2)	yes	3.9(4)	no	5.7(6)
β-residue $C_\beta H(i)$−α-residue NH(i+3)	yes	3.6(14)	yes	2.7(9)
α-residue $C_\alpha H(i)$−β-residue NH(i+3)	yes	3.8(4)	yes	4.1(6)
α-residue $C_\alpha H(i)$−β-residue $C_\alpha H$ (i+3)	no	5.4(4)	yes	3.6(4)
β-residue $C_\beta H(i)$−β-residue NH(i+4)	no	6.2(11)	yes	3.4(7)
α-residue $C_\alpha H(i)$−α-residue NH(i+4)	no	7.1(2)	yes	4.2(4)

[a] "Yes" indicates that NOEs of this type should be observed in solution if the indicated helix is formed. "No" indicates that the indicated helix would not give rise to this type of NOE. [b] The number in parentheses indicates number of measured and averaged distances.

The proposed length-dependence of helix preference among α/β-peptides is strongly supported by the crystallographic data discussed here. The length effect in our structure set is very distinct. All 11 α/β-peptides that contain 8 residues or fewer are 11-helical in the solid state, while all 3 α/β-peptides that contain 9 residues or more are 14/15-helical. The observation of a single 14-membered-ring hydrogen bond in octamer **8b**, and perhaps another in **8c**, seems to hint that the allure of the 14/15-helical conformation becomes just barely perceptible at this length, at least within this particular set of α/β-peptides (Figure 2b). Of course, it is precarious to extrapolate from conformational behavior observed in crystal structures to conformational behavior in solution, but the size of our data set and the clarity of the trend suggest that such extrapolation is reasonable in this case.

Relationships between H···H Distances and Conformationally Diagnostic NOEs. Table 1 lists the nine types of medium-range NOEs between backbone protons that have been observed for α/β-peptides containing ACPC and similarly constrained β-residues.[3a] On the basis of simple computational modeling, we previously proposed that five of these NOE patterns, three involving *i*,*i*+2 sequence relationships and two involving *i*,*i*+3 sequence relationships, could arise from either the 11-helix or the 14/15-helix, but that the other four NOE patterns would originate from only one helix or the other. Specifically, we proposed that *i*,*i*+2 α-residue $C_\alpha H \rightarrow$ α-residue NH NOEs would be characteristic of the 11-helix and that *i*,*i*+3 α-residue $C_\alpha H \rightarrow$ β-residue $C_\alpha H$, *i*,*i*+4 β-residue $C_\beta H \rightarrow$ β-residue NH, and *i*,*i*+4 α-residue $C_\alpha H \rightarrow$ α-residue NH NOEs would be characteristic of the 14/15-helix. These hypotheses constitute powerful tools for interpretation of α/β-peptide NOE data in terms of helical folding.

The crystallographic data allow incisive tests of the previously proposed relationships between backbone NOE patterns and specific helical conformations of α/β-peptides. For each type of medium-range NOE, Table 1 provides the average of all the relevant H···H distances among our 14 structures and the number of measurements contributing to

(11) (a) Baker, E. N.; Hubbard, R. E. *Prog. Biophys. Mol. Biol.* **1984**, *44*, 97. (b) Yang, J.; Gellman, S. H. *J. Am. Chem. Soc.* **1998**, *120*, 9090. (c) Yang, J. H.; Christianson, L. A.; Gellman, S. H. *Org. Lett.* **1999**, *1*, 11.
(12) (a) Bolin, A. K.; Millhauser, G. L. *Acc. Chem. Res.* **1999**, *32*, 1027. (b) Carlotto, S.; Paola, C.; Zerbetto, M.; Franco, L.; Corvaja, C.; Crisma, M.; Formaggio, F.; Toniolo, C.; Polimero, A.; Barone, V. *J. Am. Chem. Soc.* **2007**, *129*, 11248. (c) Crisma, M.; Saviano, M.; Moretto, A.; Broxterman, Q. B.; Kaptein, B.; Toniolo, C. *J. Am. Chem. Soc.* **2007**, *129*, 15471.
(13) McDonald, I. K.; Thornton, J. M. *J. Mol. Biol.* **1994**, *238*, 777.

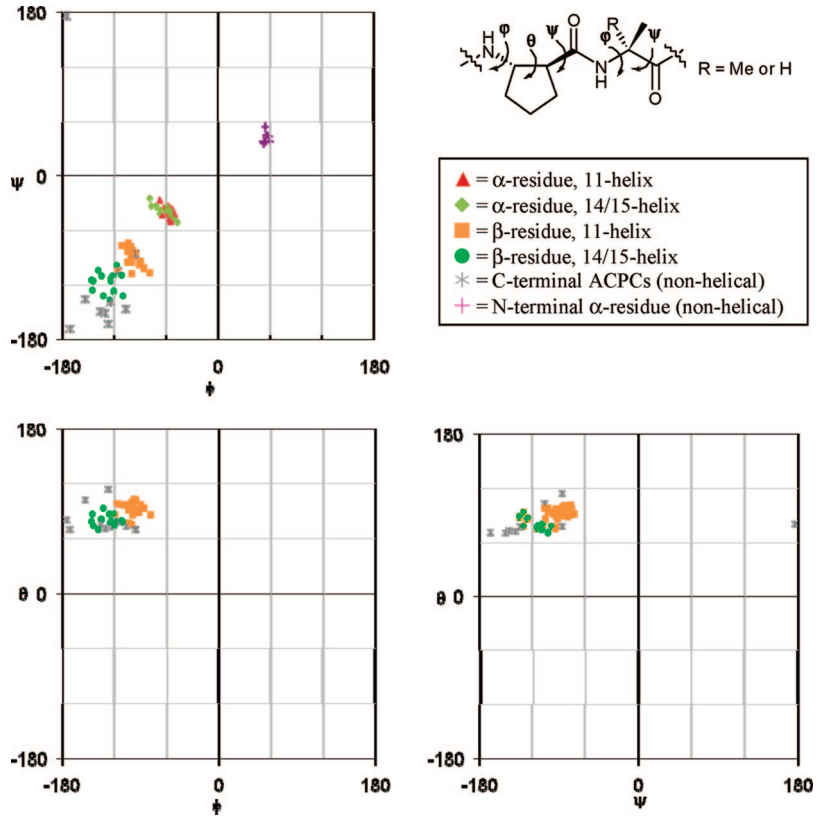

Figure 4. Ramachandran-type plots for α/β-peptides.

this average. (It should be noted that an H···H pair was included in this analysis only if both of the H atoms occurred within a helical conformation; H atoms on nonhelical N-terminal residues of **6**, **6a**, **6b**, **7a**, and **10** were not included.) In each case, our earlier deductions from modeled structures have been borne out. Thus, for example, the *i*,*i*+2 α-residue $C_\alpha H \rightarrow$ α-residue NH NOE pattern appears to arise exclusively from the 11-helix, because the four relevant H···H pairs among the 11-helical crystal structures have an average separation of 3.9 Å, which is within the NOE detection range of ~5 Å, while the six relevant H···H pairs among the 14/15-helical crystal structures have an average separation of 5.7 Å, which is too long for NOE detection. Overall, these results provide a retrospective validation of earlier NOE-based conformational analyses of 1:1 α/β-peptides and a firm foundation for analogous future studies.

Backbone Torsion Angle Analysis. The set of 14 α/β-peptide crystal structures allows us to identify average backbone torsion angles for both α-residues and β-residues in the 11-helical and 14/15-helical conformations. The data are presented in Ramachandran-type plots[14] in Figure 4, and the average torsion angles are summarized in Table 2. β-Residues have an additional torsion, corresponding to rotation about the $C_\alpha - C_\beta$ backbone bond, relative to α-residues; this torsion-distinctive β-residue torsion angle has been designated θ.[2a] The φ and ψ torsion angles of β-residues, corresponding to rotations about $N - C_\beta$ and $C_\alpha - C(=O)$, respectively, are defined by analogy to the φ and ψ torsion angles of α-residues. Because there are three torsion angles of interest for each β-residue, the graphical summary includes three two-dimensional Ramachandran-type plots so that information on all three torsion angles is available.

Table 2. Average Backbone Torsion angles (deg)

			11-helix[b]		14/15-helix[b]	
	3_{10}-helix[a]	α-helix[a]	α-residue	β-residue	α-residue	β-residue
φ	−49	−58	−56 (25)	−99 (27)	−62 (16)	−129 (14)
ψ	−26	−47	−40 (25)	−88 (27)	−38 (16)	−117 (14)
θ				93 (27)		81 (14)

[a] Reference 14. [b] The number in parentheses indicates number of measured and averaged angles.

The φ and ψ torsion angles of each helical α-residue fall in the standard α-helical region of the Ramachandran plot, with no apparent distinction between 11- and 14/15-helical α-residues. (The few α-residues that do not participate in helical conformations, because of distortion at α/β-peptide termini, are not included in this analysis.) In contrast to the similarity among α-residue torsion angles, the β-residue torsion angles differ in small but distinct ways between the two helical conformations. This difference is smallest, ~10° on average, for the θ torsion angle, which is constrained by the cyclopentane ring. The β-residue φ and ψ torsion angle averages differ by ~30° between the 11- and 14/15-helices. Overall, these results suggest that it might be possible to achieve higher stability for either helix, and higher preference for one over the other, by additional preorganization of the β-residues.

Helical Parameter Analysis. Average parameters for both 11- and 14/15-helices were deduced from the 14 crystal structures. Every helical parameter was calculated from a set of four

(14) Ramachandran, G. N.; Sasisekharan, V. *Adv. Protein Chem.* **1968**, *23*, 283.

Table 3. Average Structural Parameters of α/β-Peptide Helices

helix type	res/turn, *n*	rise/turn, *p* (Å)	rise/res, *d* (Å)	radius, *r* (Å)
11-helix	2.8	5.6	2.0	2.1
14/15-helix	3.6	5.0	1.4	2.6
3_{10}-helix[a]	3.2	5.8	1.8	2.0
α-helix[a]	3.5	5.4	1.5	2.3

[a] Reference 13; mean values in globular proteins.

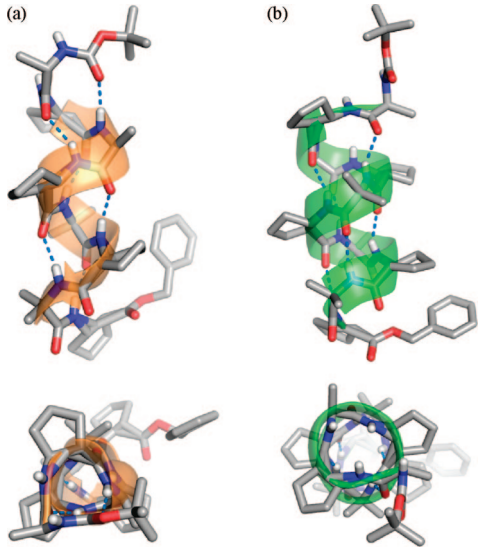

Figure 5. Cartoon representation of α/β-peptide helices: (a) 11-helix (orange, **8a**) (b) 14/15-helix (green, **10**). Views perpendicular (top) or along (bottom) the helical axis.

consecutive α-carbons by a previously reported method.[15] Only helical backbone α-carbons were used for these calculations. For β-residues, the midpoint between C_α and C_β atoms was used as an imaginary atom for the calculations. Average helical parameters are listed in Table 3. Trends between the 11- and 14/15-helices are analogous to those between the 3_{10}-helix and α-helix. For example, the number of residues per turn (*n*) of the 11- and 14/15-helices is 2.8 and 3.6, respectively, while the parameters for 3_{10}- and α-helices are 3.2 and 3.5.[13] The 11-helix has a longer rise per residue (*d*) and shorter helix radius (*r*) than the 14/15-helix (Figure 5), and comparable differences are observed between the 3_{10}- and α-helices.

Conclusions. The large set of α/β-peptide crystal structures reported here shows that use of β-residues with a five-membered-ring constraint and *trans* disposition of the amino and carboxyl groups promotes folding into two distinct helical conformations, which contain either *i*,*i*+3 or *i*,*i*+4 C=O···H−N hydrogen bonds. None of the 14 crystal structures display an alternative "hybrid" helix containing bifurcated hydrogen bonds, which suggests that this hypothetical conformation does not occur in solution. Length-dependent variations in helical conformation are consistent with the conclusion previously deduced via NMR that the *i*,*i*+4 hydrogen-bonding pattern is favored for longer α/β-peptides. Analysis of key H···H distances in the crystal structures validates conclusions regarding α/β-peptide folding in solution that were previously drawn from NOE analysis. Overall, this set of high-resolution structures should facilitate function-based design of α/β-peptides.

(15) (a) Sugeta, H.; Miyazawa, T. *Biopolymers* **1967**, *5*, 673. (b) Kahn, P. C. *Comput. Chem.* **1989**, *13*, 185.

Experimental Section

General Procedure for Dipeptide Segment Preparation. Dipeptide segments Boc-Ala-ACPC-OH (**11**) and Boc-Aib-ACPC-OH (**12**) were prepared by the previously reported procedure.[3j] The known ACPC intermediate (1 equiv), ethyl (1*S*,2*S*)-2-[(1′*S*)-phenylethyl]aminocyclopentane carboxylate hydrochloride,[10b,c] was dissolved in methanol. The mixture was shaken on a Parr apparatus under H_2 (50 psi) with 10% Pd/C (50 wt %) for 48 h. After the reaction was complete, the mixture was filtered through Celite, and the filtrate was concentrated to give the HCl salt form of *trans*-2-aminocyclopentane carboxylate (1 equiv), which was added directly to a solution of Boc-Aib-OH or Boc-Ala-OH (1 equiv), EDCI (1.5 equiv), HOBt (1.3 equiv), and DIEA (1.2 equiv) in DMF. The resulting solution was stirred for 60 h. The mixture was diluted with excess amount of EtOAc, washed with aqueous 10% citric acid, aqueous saturated $NaHCO_3$, and brine. The organic layer was dried over $MgSO_4$ and concentrated to give a crude product, which was purified by silica gel column chromatography to give the desired dipeptide ethyl ester, Boc-Aib-ACPC-OEt (**13**) or Boc-Ala-ACPC-OEt (**14**).

Boc-Aib-ACPC-OEt (13). ^{1}H NMR (300 MHz, $CDCl_3$): δ 6.70 (br s, 1H), 4.85 (br s, 1H), 4.35 (quintet, J = 7.2 Hz, 1H), 4.13 (q, J = 7.1 Hz, 2H), 2.62 (q, J = 7.9 Hz, 1H), 2.20−1.50 (m, 6H), 1.47 (s, 3H), 1.46 (s, 3H), 1.44 (s, 9H), 1.24 (t, J = 7.1 Hz, 1H). ESI-TOF MS: *m/z* 343.4 $[M + H]^+$, 365.4 $[M + Na]^+$, 707.7 $[2M + Na]^+$.

Boc-Ala-ACPC-OEt (14). ^{1}H NMR (300 MHz, $CDCl_3$): δ 6.34 (br s, 1H), 5.04 (br s, 1H), 4.37 (quintet, J = 7.5 Hz, 1H), 4.14 (q, J = 7.1 Hz, 2H), 4.19−4.03 (m, 1H), 2.60 (q, J = 8.1 Hz, 1H), 2.20−1.67 (m, 6H), 1.44 (s, 9H), 1.33 (d, J = 6.8 Hz, 1H), 1.24 (t, J = 7.1 Hz, 1H). ESI-TOF MS: *m/z* 329.4 $[M + H]^+$, 351.4 $[M + Na]^+$, 679.7 $[2M + Na]^+$.

Dipeptide segment (**13** or **14**) (1 equiv) was dissolved in MeOH/H_2O (v/v = 2:1) to generate a 0.1 M solution. $LiOH \cdot H_2O$ (5 equiv) was added at 0 °C, and the mixture was stirred for 6 h at 0 °C. After most of the solvent was evaporated by a nitrogen gas stream, aqueous 1 M HCl was added until pH ∼2. The turbid mixture was extracted with EtOAc, and the organic fraction was washed with brine, dried over $MgSO_4$, and concentrated in vacuo to give the carboxylic acid form of the dipeptide segment (**11** or **12**), which was used in peptide coupling reactions without further purification.

General Procedure for Peptide Synthesis. To a solution of amine (1 equiv) and acid (1 equiv) in DMF (∼0.1 M) were added EDCI (1.5 equiv) and DMAP (1.1 equiv). The mixture was stirred at rt for ∼60 h. Workup and purification methods were similar to those described for dipeptide segment preparation.

Boc-Aib-ACPC-Aib-ACPC-Aib-OBn (5). Boc-Aib-ACPC-OH (**11**) was coupled with HCl·H-Aib-OBn by the general procedure described above to give Boc-Aib-ACPC-Aib-OBn (**15**). ^{1}H NMR (300 MHz, $CDCl_3$): δ 8.06 (br s, 1H), 7.38−7.23 (m, 5H), 6.58 (br s, 1H), 5.13 (ABq, J_{AB} = 12.6 Hz, $\Delta\upsilon$ = 0.06 ppm, 2H), 4.80 (br s, 1H), 4.11 (m, 1H), 2.58 (m, 1H), 2.12 (m, 1H), 1.93−1.58 (m, 6H), 1.55 (s, 3H), 1.54 (s, 3H), 1.46 (s, 3H) 1.43 (br s, 12H). ESI-TOF MS: *m/z* 490.5 $[M + H]^+$, 512.5 $[M + Na]^+$, 1001.9 $[2M + Na]^+$.

Tripeptide **15** (1 equiv) was treated with 4.0 M HCl in dioxane (∼10 equiv). The mixture was stirred for 30 min and then concentrated under a nitrogen gas stream to give the HCl salt form of the amine, which was coupled with Boc-Aib-ACPC-OH by a general coupling method to give the desired product **5**. The X-ray quality crystal was grown from a chloroform/ether/*n*-heptane mixture. ^{1}H NMR (300 MHz, $CDCl_3$): δ 7.86 (d, J = 8.6 Hz, 1H), 7.76 (s, 1H), 7.39−7.22 (m, 6H), 6.51 (d, J = 8.9 Hz, 1H), 5.58 (s, 1H), 5.16 (ABq, J_{AB} = 10.0 Hz, $\Delta\upsilon$ = 0.07 ppm, 2H), 4.35 (quintet, J = 8.1 Hz, 1H), 4.26 (quintet, J = 8.6 Hz, 1H), 2.67 (q,

J = 7.6 Hz, 1H), 2.22−1.63 (m, 13H), 1.60 (s, 3H), 1.55 (s, 3H), 1.51 (s, 3H), 1.48 (s, 3H), 1.46 (s, 9H), 1.39 (s, 3H), 1.37 (s, 3H). ESI-TOF MS: *m*/*z* 686.8 $[M + H]^+$, 708.8 $[M + Na]^+$, 1394.7 $[2M + Na]^+$.

Other α/β-peptides were prepared by segment coupling analogous to those described above. Characterization data may be found in the Supporting Information.

Acknowledgment. This work was supported by the NSF grant CHE-0551920. S.H.C. was supported in part by a fellowship from the Samsung Scholarship Foundation. X-ray equipment purchase was supported in part by grants from the NSF.

Supporting Information Available: Characterization data, crystallographic information, full table of helical parameters. This material is available free of charge via the Internet at http://pubs.acs.org.

JA800355P